Laser Measurements on Nonpremixed H_2-Air Flames for Assessment of Turbulent Combustion Models

Michael C. Drake, Robert W. Pitz, and Marshall Lapp
General Electric Company, Schenectady, New York

I. Introduction

MOST practical combustion devices are turbulent nonpremixed flames. The development of appropriate computer models[1-3] for practical combustors holds the potential for their computer-aided design with lower development costs, higher fuel efficiencies, lower emissions, and wider fuel specifications. However, to be reliable over a wide range of conditions, such models should be based upon a fundamental, quantitative understanding of fuel/air mixing and chemical reactions. Considerable progress has been made in modeling fuel/air mixing processes (particularly in larboratory-scale turbulent nonpremixed flames) using probability density functions (pdf) of a conserved scalar variable to account for turbulent fluctuations[1-4] and Favre averaging to account for density variations.[5] However, the empirical correlations used in the model still rely on comparisons with experiments in nonreacting flows. A better understanding of the analogies between reacting and nonreacting flows and their deviations can result from detailed experiment/modeling comparisons in turbulent nonpremixed flames. Measurements of at least some of the key model variables (such as pdf's of conserved and reactive scalars, Favre and conventional averages and fluctuations, intermittency, extent of reaction, scalar fluxes, gradients, and correlations) are useful to directly test the model assumptions. This level of understanding is required to model turbulent chemistry interactions realistically or to predict in a fundamental way the stability limits (blowoff and relight) or the formation and emission of pollutants such as carbon monoxide and nitric oxide.[3]

Because of the problems in making detailed measurements in practical combustors and the difficulties in modeling their complex geometries and flow patterns, the development and testing of quantitative combustion models is based upon detailed comparisons with quantitative experimental data in well-controlled, laboratory-scale, nonpremixed flames operated over a range of known initial conditions. However, few comprehensive measurements have been attempted even in laboratory-scale nonpremixed flames because of the difficulties in obtaining data having sufficient temporal and spatial resolution, without significantly perturbing the flame under study. Fortunately, recent advances in laser measurement techniques[6] and, in particular, in pulsed Raman scattering, laser velocimetry, and fluorescence imaging have greatly expanded the experimental capabilities to make nonperturbing quantitative measurements in nonpremixed reacting flows.

This paper summarizes detailed experiments reported previously[4,7-12] and presents new experimental results characterizing four H_2-air jet diffusion flames. Admittedly, H_2 jet diffusion flames do not possess some elements of practical combustor systems (e.g., swirl, recirculation, com-

Michael C. Drake is a Chemist in the Fluid Mechanics Branch at the General Electric Corporate Research and Development Center. He has collaborated on the development of pulsed Raman scattering, single-pulse OH saturated fluorescence, and planar OH imaging techniques and on the application of these techniques for understanding the interactions of chemical kinetics and fluid mechanics in turbulent combustion. Previously, he was a National Research Council-National Bureau of Standards Postdoctoral Research Associate (1977-1978). He received B.S. and Ph.D degrees in chemistry from Iowa State University and Pennsylvania State University in 1970 and 1977, respectively.

Robert W. Pitz is currently an Assistant Professor at Vanderbilt University in the Department of Mechanical and Materials Engineering where he is performing research in combustion and high speed flows using laser-based diagnostics. Previously, he was a Staff Scientist at General Electric Research and Development where he investigated turbulent combustion with laser-induced Raman scattering and OH fluorescence techniques. He received a B.S. degree from Purdue University in 1973, and M.S. and Ph.D degrees from the University of California at Berkeley in 1975 and 1981. He is a Member of the American Institute of Aeronautics and Astronautics, the Optical Society of America, and the American Society of Mechanical Engineers.

Marshall Lapp is currently Supervisor of the High Temperature Interfaces Division at Sandia National Laboratories, Livermore, California. His work is focused on the effect of combustion and other high-temperature environments on immersed materials. He worked previously, for over 20 years, at the General Electric Research and Development Center, the last half of which was largely devoted to developing Raman scattering and other optical diagnostics for application to flame and fluid mechanic studies. He is a Fellow of the American Physical Society, the Optical Society of America, and the Institute of Physics (UK), and is a Member of the American Institute of Aeronautis and Astronautics, the Combustion Institute, the American Association for the Advancement of Science, and Sigma Xi. He received B.S. and Ph.D degrees from Cornell University and Caltech in 1955 and 1960, respectively.

Presented as Paper 84-0544 at the AIAA 22nd Aerospace Sciences Meeting, Reno, NV, Jan. 9-12, 1984; received Dec. 13, 1984; revision received April 5, 1985.

plex geometries, sprays, hydrocarbon kinetics). However, they do contain key aspects of turbulence/chemistry interactions (i.e., turbulent fluctuations, high heat release, and large density variations) in a simple system where the turbulent fluid mixing and the chemistry are reasonably well known as separate issues. Thus, they are ideal for investigating the effects of turbulent mixing on chemistry and, in turn, the effect of chemical heat release on turbulent mixing and are, therefore, useful for analyzing models that include these effects.

Three aspects of this work are emphasized:

1) Data suitable for detailed model comparison are presented from a variety of experimental laser-based techniques on the three types (laminar, transitional, and turbulent) of H_2 jet diffusion flames in a coflowing airstream. The data include the initial conditions, the qualitative and quantitative imaging (schlieren, shadowgraph, and planar OH fluorescence), and the probability density functions of velocity (laser velocimetry), temperature, density, major species concentrations, and mixture fraction (Raman). Favre (density weighted) and conventional means and variances are determined along with intermittency and conditional means and variances.

2) The data are analyzed to address specific modeling issues such as the importance of "coherent" structures, reaction zone shapes, intermittency, and conditional averaging. Qualitative differences between nonreacting and reacting jets are assessed with regard to scale size, half-widths, averages, and fluctuation intensities of reactive and conserved scalars, pdf shapes, intermittency, and conditional averaging.

3) Correlations of temperature and major species concentrations and comparison with simple thermodynamic models are used to demonstrate that two processes (differential diffusion and finite-rate chemistry) are important in these flames.

II. Combustor Design and Initial Condition Measurement

A jet diffusion flame combustor has been designed for these fundamental studies on nonpremixed combustion.[7,8,12] The combustor provides reproducible, well-characterized nonpremixed flames, large optical access with little optical distortion for laser diagnostic techniques, access ports for measurements requiring solid probes, and three dimensions of translational motion for flame profile studies with fixed-bed optics. The configuration of a central jet of hydrogen fuel surrounded by a coflowing stream of air was chosen because it:

1) Provides well-characterized and reproducible mixing generated by shear turbulence between the two gas streams.

2) Permits variation of turbulence levels by changing the initial velocities of the gas streams.

3) Is amenable to relatively simple theoretical fluid mechanic modeling techniques because the flow is parabolic with well-defined inlet conditions.

4) Provides simplified chemical kinetics through use of H_2 fuel.

5) Has been studied extensively by physical probe techniques (as, for example, by Kent and Bilger[13,14]).

Since the characteristics of the turbulent diffusion flame combustor have been discussed in previous publications,[7,8,12] only a few details are given here. The combustor tunnel utilized has a 3.2 mm i.d. fuel tube centered axially in a 15×15 cm square by 1 m long test section. The fuel velocity is controlled by calibrated critical flow orifices and the velocity of the surrounding, coflowing airstream by a servocontrol on the exhaust fan. The rms turbulence in the airflow was found to be acceptably low ($\sim 0.2\%$) by hot-wire anemometry. The test section and some of the laser Doppler velocimeter (LDV) and Raman instrumentation are shown in Fig. 1. The use of four flat Pyrex windows provides a maximum clear viewing area with a minimum of optical distortion for schlieren, shadowgraph, and fluorescence imaging. The test section (along with the inlet section) have been made moveable in three dimensions in order to permit flame profile studies using LDV and Raman techniques with fixed optic arrangements. This choice facilitates maintenance of the demanding optical alignment and tracking required, particularly for experiments where both laser velocimetry and pulsed Raman measurements are used simultaneously. Positioning accuracy of ~ 0.2 mm is obtained using precision screw drives and dial indicator readouts.

The Pyrex windows in Fig. 1 are mounted in aluminum frames that can be easily removed. Additional frames contain aluminum plates with ~ 5 cm diam Suprasil windows or a segmented 0.1×0.89 m quartz window for ultraviolet fluorescence imaging, a series of pressure taps for axial pressure drop measurements, or ports for inserting physical probes (hot-wire anemometers, thermocouples, gas sampling probes). Physical probes can also be inserted through the combustor sidewalls downstream of the Pyrex windows, as shown in Fig. 1.

The measured initial conditions for the four H_2-air diffusion flames investigated are summarized in Table 1. The average velocity of the fuel jet $\bar{U}_j$ is determined from volumetric flow measurements using calibrated critical flow orifices. The exit axial velocity of the jet at the flame centerline $(\bar{U}_j)_c$ and the inlet velocity of the airstream $\bar{U}_a$ are determined from radial profiles of axial velocity and fluctuation intensities measured 1 mm downstream of the fuel tip $(x/d = 0.3)$ using laser velocimetry. The tunnel air velocity profile is flat to within $\pm 2\%$. The measured jet exit velocity profiles for the $Re = 1600$ and 5200 flames are similar to those expected for laminar and turbulent pipe flow, respectively (i.e., the ratios of the centerline velocity to the average jet velocity are 2.0 and 1.4 compared to expected values of 2.0 and 1.3).[15]

The exit velocity profile of the jet was not measured in the $Re = 8500$ flame because the high expected centerline velocity ($U_c \sim 1.3\ \bar{U}_j = 370$ m/s) and its correspondingly high Doppler frequency made such measurements unreliable. Based upon the $Re = 5200$ profile results, the $Re = 8500$ initial profile

Table 1 Flow conditions for hydrogen/air flames

Re	Flame type	$\bar{U}_j$, m/s	$\bar{U}_a$, m/s	$\bar{U}_j/\bar{U}_a$	dp/dx, (Pa/m)
660	Laminar	22	9.3	2.4	~0
1600	Transitional	53.6	8.8	6.1	−10
5200	Turbulent	174.2	13.3	13	−32
8500	Turbulent	285	12.5	22.8	−51

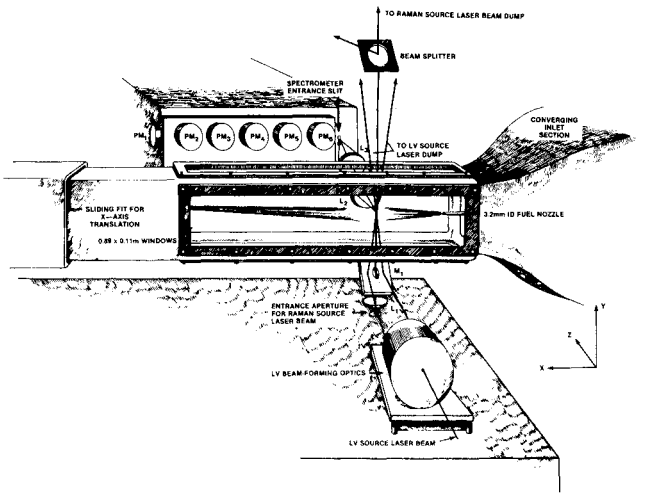

Fig. 1 Combustor test section with laser velocimetry and Raman scattering optics.

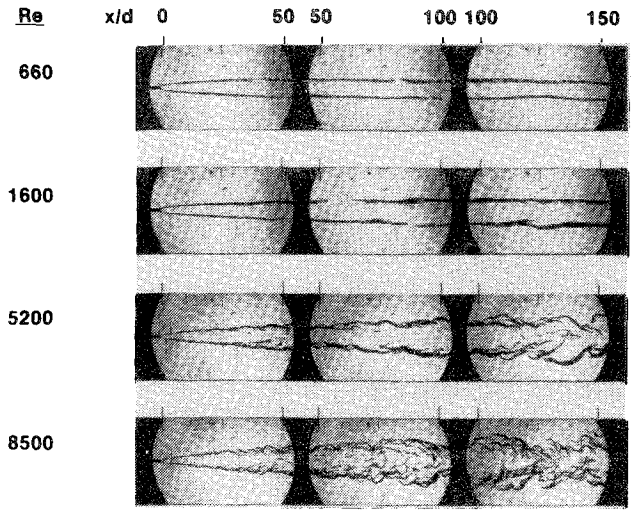

Fig. 2 Pulsed laser schlieren images of nonpremixed H_2/air flames studied showing laminar ($Re=660$), transitional ($Re=1600$), and turbulent ($Re=5200$ and 8500) flame structure.

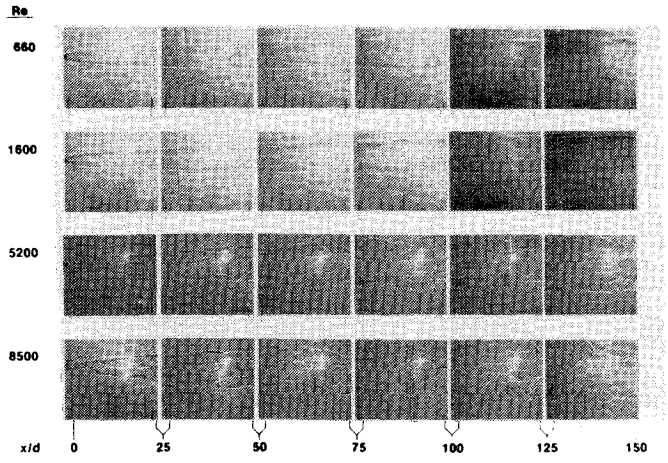

Fig. 3 Pulsed laser shadowgraph images of nonpremixed H_2/air flames.

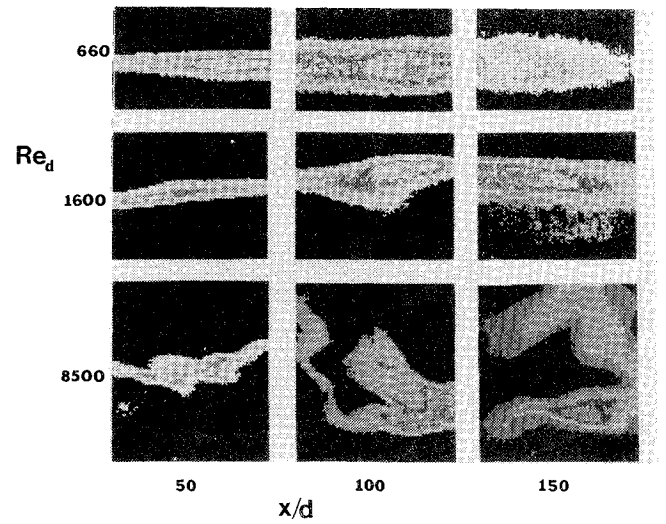

Fig. 4 Planar OH images of reaction zone structures in nonpremixed H_2/air flames (gray scale indicates relative molecular OH concentration). The bottom of each frame corresponds to the combustor centerline and the image viewed is 30×30 mm; each pixel corresponds to a volume of $0.3\times0.3\times0.4$ mm. Color photographs are shown in Ref. 9.

should have close to a turbulent pipe flow profile as well.

The axial pressure gradients were measured by a series of 14 wall pressure taps on the combustor centerline. The pressure gradient measurements were checked by LDV measurements of the gradient in the freestream velocity U_{fs} using the expression for conservation of momentum along the axial dimension x,

$$dp/dx=\rho U_{fs}dU_{fs}/dx \tag{1}$$

assuming inviscid fluid and no transverse velocity gradients. The computed pressure gradient determined by Eq. (1) for the $Re=8500$ flame was -49 Pa/m, which is in agreement with the value -51 Pa/m measured by the pressure taps.

III. Flame Imaging Results

Imaging techniques (schlieren, shadowgraph, and planar OH fluorescence) were used to characterize the four flames qualitatively. Schlieren images are shown in Fig. 2 with each image corresponding to a 100×150 mm area. The central fuel tube is visible in each farthest left photograph. The shadowgraph photos in Fig. 3 correspond to a smaller 75×80 mm imaged area. Each schlieren and shadowgraph image was obtained with a 1 μs exposure from a laser pumped by a flash lamp.

The laminar structure of the $Re=660$ flame close to the fuel nozzle is clearly evident in both the schlieren and shadowgraph photos, but far downstream some instabilities are observed. The transitional flame ($Re=1600$) shows an initial laminar region with a sharp break (most evident in the schlieren photo) at $x/d\sim40$ followed by a more turbulent region. Schlieren movies indicate that the transition point rapidly fluctuates from $12\leq x/d\leq50$. The time-averaged induction length from these data is 34 diam, in agreement with the 28 diam value measured by Takeno and Kotani[16,17] at the same Reynolds number. Although both the $Re=5200$ and 8500 flames are turbulent, there is a marked decrease in turbulence length scales in the higher Reynolds number flame. Attempts to further increase the H_2 flow velocity resulted in flame blowoff.

In nonreacting flows (i.e., substituting helium for the hydrogen fuel), the schlieren images show much smaller scale sizes in turbulent flows and a much shorter induction length in transitional flows, in agreement with similar observations by Takeno and Kotani.[17] The results are in accord with the suggestions by Hottel and Hawthorne[18] that combustion changes jet flame structure by increasing viscosity and decreasing the Reynolds number. Therefore, heat release during combustion results in "laminarization" of transitional and turbulent jet diffusion flames.[19]

Although schlieren and shadowgraph images provide qualitative indications of flame type and scale size, the relationship of these data to quantitative information is made complicated by the line-of-sight averaging of these techniques. For a more quantitative visualization of reaction zones in these flames, planar laser induced fluorescence of OH molecules is used.[9] The OH molecules are excited by a thin (<0.4 mm) sheet of light from a single pulse (10 ns, 3 mJ) of a dye laser tuned to a specific OH absorption frequency (310 nm) and detected using a two-dimensional image-intensified photodiode array camera. The intensity of the fluorescence is approximately proportional to the concentration of OH molecules present. Since OH molecules are predominately found in reaction zones of nonpremixed flames, planar OH fluorescence is an excellent indicator of reaction zone locations and shapes.

Representative examples of OH images in the laminar and turbulent flames are shown in Fig. 4. The optics were arranged so that the camera viewed an area of 30×30 mm and the viewing field was adjusted so that the bottom edge of each view corresponded with the centerline of the flame. Thus, each element of the 100×100 array detector detected OH fluorescence from a sample volume of $0.3\times0.3\times0.4$

mm. The maximum OH levels (light areas) correspond to approximately 6×10^{16} molecules/cm^3.

Figure 4 shows representative images from each of the three flames at each of the three positions investigated. Comparing the results of many different images at the same flame location demonstrates that laminar flames give smooth reaction zones that have little variation in width or position. The turbulent flame shows markedly different reaction zone shapes, widths, and positions from one measurement to the next. The most probable reaction zone width is smaller in the turbulent flame than in the laminar flame (i.e., ~2.1 vs ~5.0 mm at $x/d=50$) because of the flame front stretching due to increased shear forces. The average reaction zone widths in each flame increase with increasing distance downstream. A continuously connected reaction zone was observed in qualitative agreement with a "stretched laminar flamelet" model[20,21] at all flame locations studied except far downstream ($x/d\sim150$) in the $Re=8500$ flame. At that flame location, approximately half of the 90 images taken indicate the absence of any continuous reaction zone from one side of the frame to the other (perhaps indicating either the breakup of the flame sheet or a burnout of the fuel).

Large-scale "coherent" (taken in this context to mean organized, regular, repetitive) structures have been experimentally observed by others[22,23] in turbulent nonreacting and reacting shear flows (i.e., mixing layers, boundary layers, and early regions of jets and wakes). Although there appears to be little controversy that large-scale structures are present in all regions of turbulent jet flames and that they can have an important influence on fuel/air mixing, the coherence of these structures in the downstream regions of turbulent jet diffusion flames remains open to question. As Yule[24] has stated. "The ease with which coherent laminar vortex-type structures can be visualized in low Reynolds number transitional or artificially stabilized turbulent flows can lead to the tempting, but often unsubstantiated, use of the data...to describe the structures of the fully turbulent regions of the same flows."

Large-scale vortex-like reaction zone shapes are observed in the OH fluorescent images of turbulent H_2 jet flames (see Fig. 4). However, the limited data that are currently available in this study[9] show no conclusive evidence for repetitive "coherent" structures in the downstream regions. In our view, the large-scale structures that are present may not be inconsistent with the classical views of turbulence[25] nor with the usual Eulerian modeling approaches. Clearly, more work using planar laser-induced fluorescence imaging as well as other laser techniques is required to determine the importance of coherent structures in turbulent reacting flows.

IV. Reactive Scalar Measurements

Laser Velocimetry

The laser velocimetry measurements were made with a dual-beam, real-fringe optical configuration, a 100 MHz period counter, and a digital oscilloscope interfaced to a minicomputer.[12] Fuel and air streams were independently seeded with nominal 1 μm diam alumina particles. The velocity measurements in the $Re=1600$ flame are 4096 point averages and those in the other flames consist of 2048 point averages.

The axial decay of excess centerline axial velocity U (defined as the average axial velocity on the centerline minus the free-stream axial velocity at the same x/d position) normalized by the initial excess velocity measured close to the nozzle at $x/d=0.3$ is shown in Fig. 5. The results are compared with the decay of Favre-averaged mixture fraction $\tilde{\xi}$ measured by Raman scattering in these flames as reported by Drake et al.[4] (Raman scattering results are discussed in more detail in the next section.) Qualitatively, in the transitional $Re=1600$ flame, the excess velocity decays more slowly than the mixture fraction. (Note, however, the rapid decay in excess velocity in the $Re=1600$ flame between $x/d=25$ and 50.)

In the turbulent $Re=5200$ and 8500 flames, the decay of excess velocity and Favre mixture fraction are nearly equal with an initial dependence of $\sim x^{-1/3}$. Farther downstream ($x/d>150$), both the excess velocity and Favre mixture fraction decay much more rapidly ($\sim x^{-5/3}$ and x^{-3}, respectively). The same trend in the centerline velocity was observed in a coflowing H_2-air jet diffusion flame by Glass and Bilger,[26] who found that the excess velocity decays in the same way as $x^{-1/3}$ in the main flame regions ($x/d=50$ to 150) and $\sim x^{-3/2}$ far downstream ($x/d>150$). These results are quite different from nonreacting turbulent round jets into still air[27] that decay as x^{-1} or from nonreacting turbulent coflowing round jets that decay like a jet initially ($\sim x^{-1}$) and then decay less rapidly as a wake downstream ($\sim x^{-1/3}$).[28-31] The decay observed far downstream in the flames is close to that measured in nonreacting plumes with a slope of $-5/3$ (see Ref. 27, pp. 32-37).

The centerline decay of axial velocity fluctuation intensity $(\overline{U'^2})^{1/2}/\tilde{U}$ is compared in Fig. 6a with the Favre-averaged mixture fraction fluctuation intensity $(\tilde{\xi}''^2)^{1/2}/\tilde{\xi}$ reported previously.[4] The turbulent $Re=5200$ and 8500 flames have a constant centerline fluctuation intensity of between 0.18 and 0.20 at $x/d\leq100$. Farther downstream ($x/d>100$), the fluctuation intensities rapidly increase. The difference between the excess velocity and Favre mixture fraction fluctuation intensities in the downstream region (see Fig. 6a) is primarily due to the density weighting (Favre averaging). For example, the conventionally averaged mixture fraction fluctuation intensities have values much closer to the conventionally averaged excess velocity fluctuation intensities in intermittent regions of the $Re=8500$ flame.

The present measurements of axial velocity fluctuation intensities in turbulent H_2 flames are shown in Fig. 6b to be in good agreement with previous measurements in turbulent jet diffusion flames with H_2[26,32-35] and with H_2/argon fuels.[36-39] In $Re=11{,}200$ H_2 flames with axial pressure gradients of -18 and -102 Pa/m, Starner and Bilger[32] measured a nearly constant value of 0.2 for excess velocity turbulent intensities in both flames at axial locations between 40 and 80 diam. Farther downstream, Starner and Bilger measured higher in-

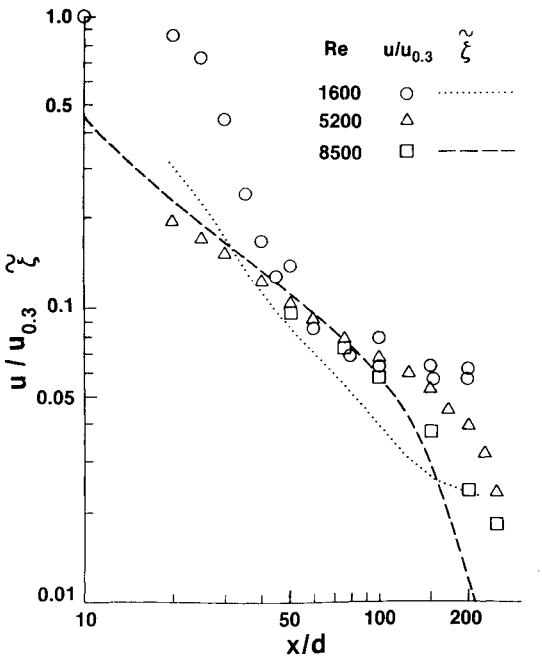

Fig. 5 Axial centerline profile of excess axial velocity u normalized by its initial value $u_{0.3}$ measured at $x/d=0.3$. Data compared to Favre-averaged mixture fraction $\tilde{\xi}$ profile in the $Re=1600$ and 8500 flames.[4]

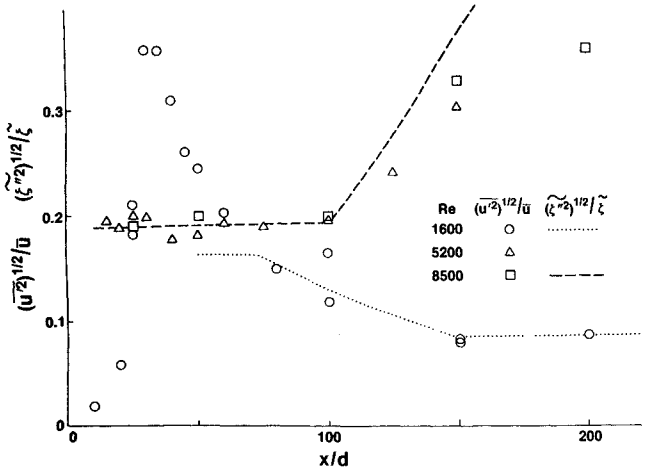

a) Data compared to fluctuation intensity of Favre-averaged mixture fraction $\tilde{\xi}$ profile in the $Re=1600$ and 8500 flames.[4]

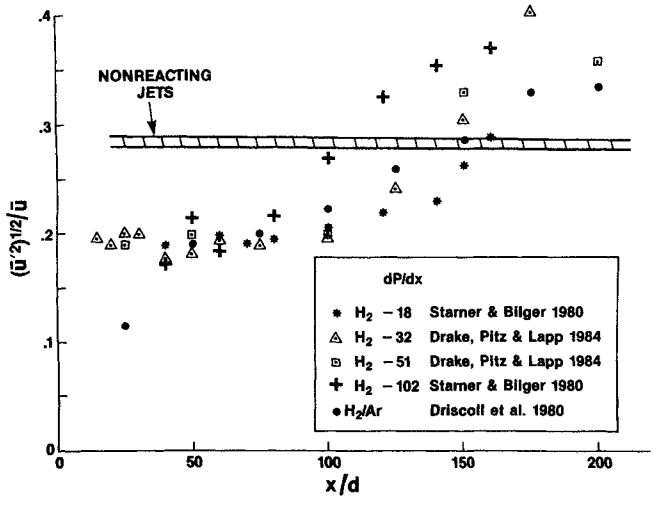

b) Data compared with fluctuation intensities of axial excess velocity measured by others in nonreacting jets and in H_2 and H_2/Ar jet flames as a function of axial pressure gradient.

Fig. 6 Axial centerline profile of the fluctuation intensity of excess axial velocity.

tensities, particularly for the flame with the more negative pressure gradient. In this downstream region of the present $Re=5200$ and 8500 flames (with axial pressure gradients of -32 and -51 Pa/m, respectively), the measured fluctuation intensities (Fig. 6b) lie between the results from the two flames studied by Bilger and Starner. The turbulence intensity measurements in a H_2/argon flame by Driscoll et al.[36] are also in excellent agreement when the difference in flame length ($x/d\sim60$ compared to ~150 in H_2 flames) is used to scale the axial distance.

The nearly constant value of 0.19 measured here at $x/d\lesssim100$ for turbulent flame axial velocity fluctuation intensities is in reasonable agreement with mixture fraction fluctuation intensities measured in the same flame by Raman scattering.[4] Somewhat larger mixture fraction fluctuation intensities (0.3-0.4) were estimated by Kent[40] from the copresence of hydrogen and oxygen in the sample probe volume of the $Re=11{,}200$ flame. The very large mixture fraction fluctuation values (≥0.4) measured by Mie scattering techniques[41] are very likely erroneous.[4]

In nonreacting turbulent jet flows into still air, the values of fluctuation intensities of excess velocity[42] and jet fluid concentrations[43] are also equal to each other, although their value tends to be higher (0.28-0.29).[27,42-45] In nonreacting, coflowing turbulent jets,[28] the centerline temperature scalar

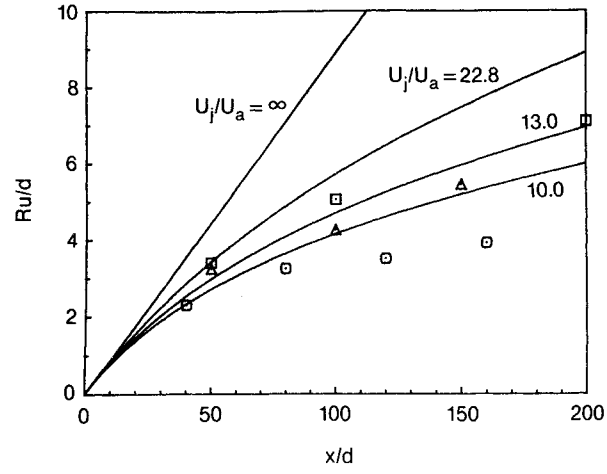

Fig. 7 Axial dependence of R_u the radius at the one-half excess velocity point. The straight line is for a jet in still air ($\bar{U}_j/\bar{U}_a=\infty$). The other solid lines are predictions for nonreacting coflowing jets according to a correlation by Abramovich[44] at three values of $\bar{U}_j/\bar{U}_a=10$, 13, 23. The data from H_2/air jet flame is: ⊡ $Re=8500$, $\bar{U}_j/\bar{U}_a=23$; △ $Re=5200$, $\bar{U}_j/\bar{U}_a=13$ from this work; and ○ $Re=11{,}000$, $\bar{U}_j/\bar{U}_a=10$ from Glass and Bilger.[26]

fluctuation intensities are 0.16-0.21, which is close to the values for fluctuation intensities found in the near field of the jet flame. The centerline velocity fluctuations in the nonreacting coflowing turbulent jets[28,45] are 0.2-0.3 in the near field (the "jet-like" zone) and increase to 0.3-0.5 farther downstream (the "wake-like" zone). The same trends are observed in the present coflowing jet flame data in Figs. 6a and 6b.

The trends in excess velocity fluctuation intensities in the transitional ($Re=1600$) flame shown in Fig. 6a are more complex. Near the jet very low values are observed, while in the region $x/d=25$-50 very high (~0.35) values are measured. Farther downstream ($x/d>50$), a smooth decay in fluctuation intensity is observed, in close agreement with that for Favre mixture fraction. The fluctuation intensities for excess velocity and Favre mixture fraction are equal to each other in this flame as well (except at $x/d=50$). Unfortunately, Raman measurements were not made at $x/d<50$ in the $Re=1600$ flame.

The trends in fluctuation intensity measured in the $Re=1600$ flame are consistent with the rate of excess velocity decay shown in Fig. 5 [i.e., shallow rates of decay at $x/d<25$ and >75 in Fig. 5 correspond to regions of low fluctuation intensity in Fig. 6a and very rapid decays ($x/d=25$-50) in Fig. 5 correspond to regions of high fluctuation intensity]. It is likely that the high fluctuation intensity is a result of axial oscillation ($x/d=12$-50) in the transition point between laminar and turbulent flow for this transitional ($Re=1600$) flame.

The variations of R_u, the half-radius of the jet at the one-half excess velocity point, for the present turbulent $Re=5200$ and 8500 flames and the $Re=11{,}000$ flame of Glass and Bilger[26] are shown in Fig. 7. The flame results are compared to a correlation developed from an integral analysis of a nonreacting coflowing jet by Abramovich (see pp. 195-197 of Ref. 44). This correlation fits the nonreacting coflowing jet data of Antonia and Bilger[45] to within $\pm5\%$ for $x/d>30$. The correlation is plotted in Fig. 7 for the velocity ratio of the three flames $\bar{U}_j/\bar{U}_0=10$, 13, and 23. The straight line shown in Fig. 7 is for the growth of a nonreacting jet into still air that has a slope of 0.0891 (mean value determined from a collection of growth data given by Rodi[27]). In all the reacting jet flames, the half-radius increases more slowly (as much as 20-25% in the far field) than in the corresponding nonreacting cases. This decrease could be due to the

laminarization in the turbulent flame zone[19] that occurs near the boundary of the H_2/air jet. This lowered growth rate due to reaction is similar to that found in a reacting shear layer formed behind a rearward facing step, where the edge of the shear layer defined by the velocity field grew more slowly into the premixed reactants with reaction than without reaction.[46] Half-radii of nonreacting coflowing jets grow as a jet ($\sim x$) initially and like a wake ($\sim x^{1/3}$) farther downstream. The power law dependencies of the growth rates from the flames shown in Fig. 7 have been analyzed and lie between these two limits. The $Re = 8500$ and 5200 flames with higher values of $\bar{U}_j/\bar{U}_0$ (23 and 13, respectively) grow like $x^{1/2}$ in the far field. The $Re = 11{,}000$ flame of Glass and Bilger[26] has a lower value of $\bar{U}_j/\bar{U}_0$ and approaches the growth rate of a wake in the far field ($\sim x^{1/3}$).

Both Favre averaged $R_{\tilde{\xi}}$ and conventionally averaged $R_{\bar{\xi}}$ mixture fraction half-radii have also been measured in the $Re = 1600$ and 8500 flames using Raman scattering. In the $Re = 8500$ flame, the measured ratio $R_{\tilde{\xi}}/R_{\bar{\xi}}$ is approximately 1 near the nozzle and ~ 0.8 downstream at $x/d > 100$. The reason for the differences in half-radii stems from the definition of Favre averaging, which is

$$\tilde{\xi} \equiv \bar{\xi} + \overline{\rho'\xi'}/\bar{\rho} \tag{2}$$

Using simultaneous Mie scattering and laser velocimetry, Starner and Bilger[35] have shown that the correlation $\overline{\rho'\xi'}$ is always negative in turbulent H_2 flames (which gives $\tilde{\xi} < \bar{\xi}$) and the ratio of $\tilde{\xi}:\bar{\xi}$ decreases at the edges of the flame (so that $R_{\tilde{\xi}} < R_{\bar{\xi}}$).

The conventionally and Favre-averaged velocity are related in a similar way,

$$\tilde{u} \equiv \bar{u} + \overline{\rho'u'}/\bar{\rho} \tag{3}$$

Starner and Bilger[35] have also shown that $\overline{\rho'u'}$ is always negative, but it has a much smaller relative value making $\tilde{u} \cong \bar{u}$ (i.e., the difference between $\tilde{u}$ and $\bar{u}$ determined from Table II in Ref. 35 is less than 4%). Therefore, the half-radii determined from $\tilde{u}$ and $\bar{u}$ should be nearly identical. Although the previously reported values of the correlation $\overline{\rho'\xi'}$ and $\overline{\rho'u'}$ may not be accurate (because Mie scattering has been shown[4] to overestimate mixture fraction fluctuations and the extent of intermittency), the relative magnitudes of $\overline{\rho'u'}$ and $\overline{\rho'\xi'}$ should be correct.

In confined turbulent nonreacting jets, Steward and Guruz[47] used the square of the measured half-radii of excess velocity and excess temperature to determine a mean effective Prandtl number (a measure of the relative rate of turbulent diffusion of momentum compared with turbulent diffusion of heat). An analogous relationship involving the half-radii of excess velocity and species concentration was used by Batt[48] to determine a mean turbulent Schmidt number for a nonreacting shear layer and by Glass and Bilger[26] in a H_2 jet flame. The only assumption used was that the normalized radial profiles of velocity and mixture fraction have the same shape.

Using this relationship for the turbulent Schmidt number Sc,

$$Sc \cong (R_{\tilde{u}}/R_{\tilde{\xi}})^2 \tag{4}$$

(and assuming that $R_{\tilde{u}} = R_{\bar{u}}$) gives an average value of ~ 0.6 for an effective turbulent Schmidt number in turbulent regions of the transitional ($Re = 1600$) flame. This is consistent with the trends in Fig. 5, where the excess velocity decays more slowly than Favre mixture fraction. The value of 0.6 measured here in a transitional flame is close to the value of 0.7 measured for the Prandtl and Schmidt numbers in nonreacting turbulent jets by numerous investigators.[27]

The results in the turbulent $Re = 8500$ flame are rather different. The excess velocity decay in Fig. 5 is close to the decay in Favre mixture fraction and measured values of

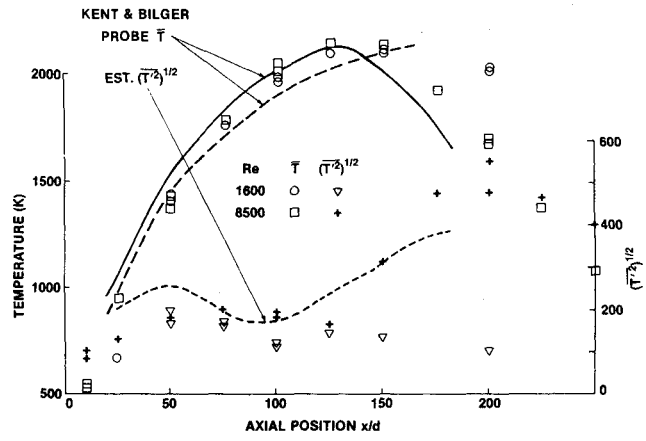

Fig. 8 Axial profile of average and rms fluctuations of temperature from pulsed Raman data compared to probe measurements of average temperatures[13,14] in —— $\bar{U}_j/\bar{U}_a = 10$ and - - - $\bar{U}_j/\bar{U}_a = 5$ flames and to estimated rms temperature fluctuation in ---- $\bar{U}_j/\bar{U}_a = 10$ flame.

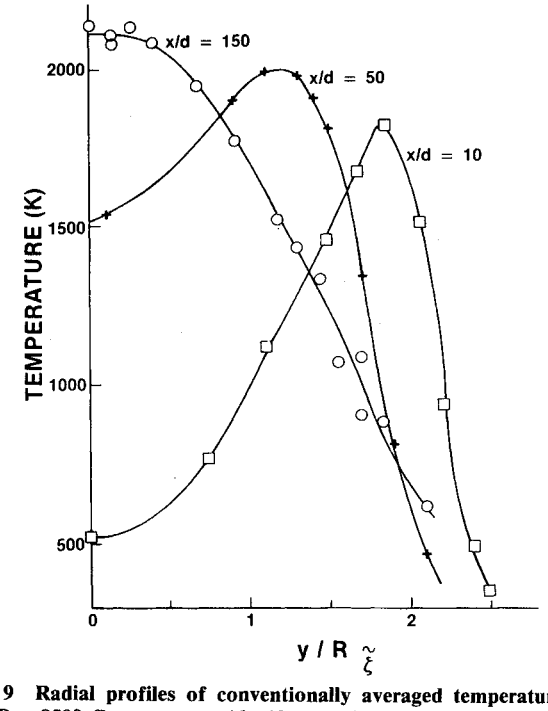

Fig. 9 Radial profiles of conventionally averaged temperature in the $Re = 8500$ flame at □ $x/d = 10$, + $x/d = 50$, and ○ $x/d = 150$. The radial distance y is normalized by the half-radius based upon Favre mixture fraction $R_{\tilde{\xi}}$.

$(R_{\tilde{u}}/R_{\tilde{\xi}})^2$ imply a turbulent Schmidt number of ~ 1.2. [Using conventional mixture fraction half-radii gives an average of 1.0 for $(R_{\bar{u}}/R_{\bar{\xi}})^2$.] Analysis of radial profiles of $\tilde{\xi}$ and $\tilde{u}$ from Raman and laser velocimetry data at $x/d = 50$ in a turbulent H_2/argon flame by Dibble et al.[38] also gives a value of 1.0 for the square of the ratio of half-radii. Glass and Bilger[26] measured Schmidt numbers of $\simeq 1$ at $x/d < 80$ and values as low as 0.7 at $x/d \geq 160$.

The value of the turbulent Schmidt number from our Raman and laser velocimetry measurements is only approximate, primarily because of difficulties in determining the half-radii from the relatively coarse spatial grid of Raman measurements. However, the data suggest a turbulent Schmidt number close to unity, rather than the value of 0.7 measured in nonreacting flows and often assumed in turbulent combustion modeling.[4,5,49] It is interesting to note that Kent and Bilger[49] get somewhat better agreement with

their H_2 flame experimental results in the outer parts of the flow using a model with Schmidt and Prandtl numbers equal to 1.0 rather than 0.7. Similar model/data comparisons in the present flames[4] using a Schmidt number of 0.7 show that diffusion of turbulence kinetic energy is underpredicted in the $Re=8500$ flame, but not in the $Re=1600$ flame. More extensive measurements are needed to clarify this issue. Indeed, it is by no means obvious that an overall average turbulent Schmidt and Prandtl number is even a meaningful concept when applied to turbulent jet flames.

Pulsed Raman Scattering

The apparatus and data reduction for pulsed spontaneous Raman scattering measurements have been discussed in detail previously.[4,10,12] A dye laser pumped by a flash lamp provides pulses of ~1 J at 488 nm to excite the Raman scattering, which is analyzed by a ¾ m spectrometer, six photomultiplier tubes, and a gated electronic detection system. For each individual laser pulse, the temperature is determined from the anti-Stokes-to-Stokes N_2 vibrational Raman scattering intensity ratio and the concentration of each of the major species (H_2, N_2, O_2, H_2O) are determined from their respective Stokes vibrational Raman intensities. Extensive calibrations of the Raman system in laminar, premixed flames indicate the Raman measurements are accurate to ±50 K for temperature[10] and ±1 mole% for species mole fraction.[12] The temporal resolutions (2 μs) of the Raman system is limited by the laser pulse length, the spatial resolution ($0.3\times0.3\times0.7$ mm) by the spectrometer entrance slit and the collection optics magnification, and the data acquisition rate (1 pps) by the laser repetition rate. Most of the Raman results reported here consist of 200 point data samples, although some 2000 point samples are included.

Because the Raman scattering diagnostic technique provides such a complete description of the thermodynamic state of the system, other instantaneous quantities such as density and mixture fraction can be calculated. Repetitively pulsing the laser at the same flame location gives direct measurements of probability density functions (pdf) for each of the scalar variables from which intermittency and conventional or density-weighted (Favre) averages, rms fluctuations, higher-order moments, and correlations can be determined.

Raman results have been reported previously for reactive scalars in the $Re=1600$ and 5200 flames[7,8] and for the conserved scalar mixture fraction[4] in all four flames. This section details reactive scalar measurements, primarily temperature in the $Re=8500$ flame, and compares them to previous probe sampling and laser results. The axial centerline profile of conventionally averaged temperature $\tilde{T}$ and its rms fluctuation $(\widetilde{T''^2})^{1/2}$ in the $Re=1600$ and 8500 flames are shown in Fig. 8. The axial profile for the $Re=8500$ flame is in reasonable agreement with thermocouple measurements by Kent and Bilger[13,14,49] on an $Re=11{,}200$ H_2 flame (with $\tilde{U}_j/\tilde{U}_a=10$). In our Raman results, the maximum average temperature on the centerline occurs at the turbulent flame length ($x/d=125$) with a value of 2100 K, which is below the adiabatic flame temperature of 2380 K due to turbulent fluctuations. The measured rms temperature values for the $Re=1600$ flame slowly decrease from a value of ~170 K at $x/d=50$ down to 110 K at $x/d=200$. In the turbulent $Re=8500$ flame, the temperature fluctuations are somewhat larger than the $Re=1600$ results at $x/d\leq125$. The values of temperature fluctuation become very large (≥500 K) at $x/d=150$—the same location at which the fluctuation in excess axial velocity and Favre mixture also increase (see Fig. 6a).

The axial profiles in $(\widetilde{T''^2})^{1/2}$ for the $Re=8500$ flame show good agreement with those estimated by Kent and Bilger[49] for their $Re=11{,}200$ H_2 flame (shown as a dotted line in Fig. 8); however, direct measurements of the temperature fluctuations in their flame have not been made. Although reliable measurements of temperature fluctuations using thermocouples are very difficult, measurements on CH_4 turbulent jet diffusion flames have been reported by Roberts and Moss[50] and by Lockwood and Moneib[51] (which supersede previous measurements[52] where the reported fluctuation levels were erroneously low). In their CH_4 flames, the maximum measured values of rms temperature fluctuations were ~500 K. Temperature fluctuations are expected to be higher in our turbulent H_2 flames because of the higher maximum flame temperature and steeper temperature gradients.

The radial profiles of $\tilde{T}$ and $(\widetilde{T''^2})^{1/2}$ in the $Re=8500$ flame at $x/d=10$, 50, and 150 are shown in Figs. 9 and 10. The maximum radial flame temperature coincides with the average position of the flame front, peaking off-axis until the flame reaches the centerline at $x/d\sim150$. The maximum flame temperature values determined from the radial profiles increase from the nozzle to $x/d=150$ (Fig. 9) and decrease thereafter (Fig. 8). The lower flame temperatures near the nozzle may be due to superequilibrium radical concentrations (discussed in Sec. VI). The trends in $(\widetilde{T''^2})^{1/2}$ are the same as those measured previously in the $Re=1600$ flame.[8] Off-axis values of $(\widetilde{T''^2})^{1/2}$ are larger than on the centerline, peaking at 550, 750, and 725 K for $x/d=10$, 50, and 150, respectively in the $Re=8500$ flame. The shapes of the radial profiles and the magnitudes of $(\widetilde{T''^2})^{1/2}$ are in agreement with Raman measurements by Dibble et al.,[38] who found peak rms temperature values of 600 K in a turbulent H_2/argon jet flame.

Radial profiles of the values of the mole fraction of H_2, N_2, O_2, and H_2O and of the density normalized by the density of room air are shown in Fig. 11 for the $Re=8500$ flame at $x/d=10$, 50, and 150. Note that the density is quite constant near the center of the flame and rises sharply at the outer edge of the flame (similar to trends seen by Schefer and Dibble[37]).

V. Probability Density Functions, Intermittency, and Conditional Averages

The reactive and conserved scalar means and rms fluctuations discussed in Sec. IV are calculated from probability density functions (histograms) that are measured directly by laser velocimetry or Raman scattering. Examples of pdf's of a reactive scalar (in this case, conventionally averaged temperatures) at various radial locations at $x/d=50$ are shown in Figs. 12 and 13 for the $Re=1600$ and 8500 flames, respectively. The pdf's in the transitional flames consist of a

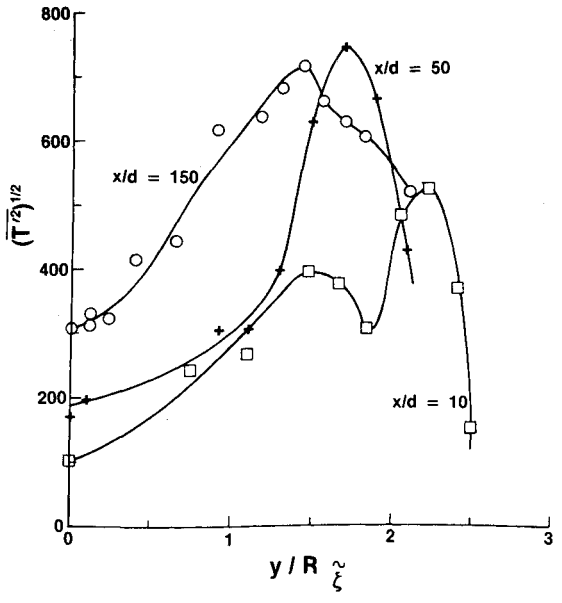

Fig. 10 Radial profiles of rms temperature fluctuations in the $Re=8500$ flame at □ $x/d=10$, + $x/d=50$, and ○ $x/d=150$.

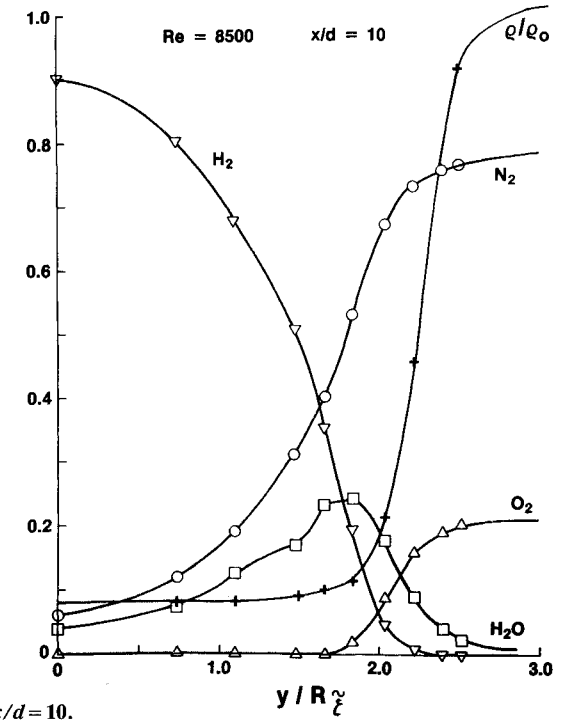

a) $x/d = 10$.

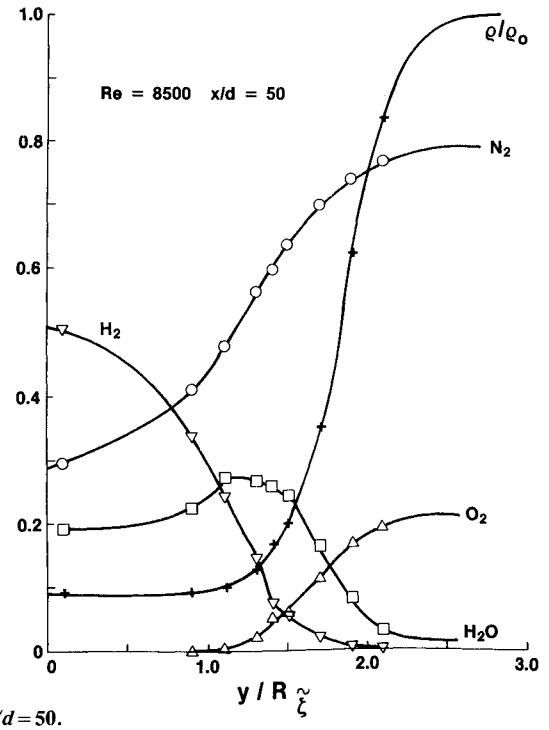

b) $x/d = 50$.

Fig. 11 Radial profiles of major species mole fractions and normalized density in the $Re = 8500$ flame.

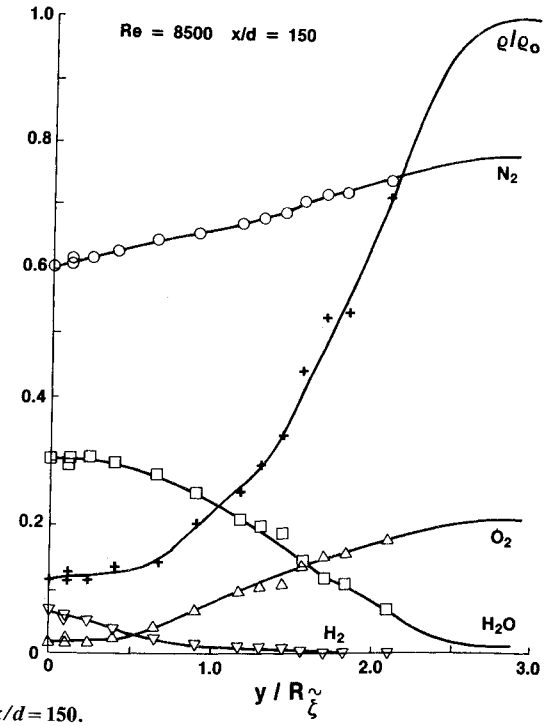

c) $x/d = 150$.

single peak similar to that found in laminar diffusion flames, except that it is considerably broader. The pdf's in the turbulent flame (Fig. 13) are qualitatively different, showing a marked bimodal distribution. The sharp spike, which becomes more pronounced for larger values of y, is due to nonturbulent uncontaminated air, while the broad peak is due to turbulent fluid. These pdf's are qualitatively similar to those of other reactive or conserved scalar variables.[4,41,53] Many turbulent mixing models for nonreacting and reacting flows are based upon these pdf's, which are assumed to consist of an intermittent spike (nonturbulent fluid) and a clipped Gaussian (turbulent fluid).

An important parameter characterizing these pdf's is the Favre-averaged intermittency $\tilde{\gamma}$, which is the density-weighted fraction of time that turbulent fluid is present at a point in the flow. Favre intermittency is mathematically defined as, $\overline{\rho I}/\bar{\rho}$, where $I(t)$ for each instantaneous measurement is zero in the freestream and one when significant turbulent jet fluid is present. For intermittency and conditional averaging measurements, the discrimination between turbulent and nonturbulent fluid should conceptually rely on the variance of the vorticity fluctuations, which is very difficult to measure. However, since the initial airstream is laminar and the hydrogen jet is initially turbulent, the presence of significant hydrogen bearing species is used to identify turbulent zones.

Preliminary results of intermittency and conditional means, rms values and pdf's have been reported earlier based on the sum of $X_{H_2O} + X_{H_2}$ as the discriminating function.[4,11] The results presented here are more accurate because the conserved scalar hydrogen element mass fraction mixture fraction ξ is used as the discriminating function, corrections are made for water vapor in the inlet airstream, and the threshold level is more systematically determined.[54] The flow is considered turbulent when $\xi \geq 0.0004$. The variation of Favre intermittency plotted on a probability scale with radial position normalized by the mixture fraction half-radius is shown in Fig. 14. As before,[4] linear behavior is observed in Fig. 14 at all axial positions except $x/d = 200$, where intermittency has reached the flame centerline. This linear behavior indicates a Gaussian time-averaged interface, which is consistent with that found by Starner[34] in a turbulent H_2 flame and by Schefer and Dibble[37] in a turbulent H_2/argon flame. This Gaussian behavior is not unique to reacting flows, having been reported in nonreacting jets[55] and wakes.[56] The difference in turbulent H_2 flames is the decrease in slope with increasing x/d, as seen in Fig. 14. This is in agreement with the results of Starner[34] and may be yet another indication of a transition from jet-like behavior close to the nozzle to wake-like far downstream (as discussed earlier). A lack of similarity in profiles of density (not shown) and intermittency (Fig. 14) that we observe here is not surprising due to the influences of the coflowing airstream and the combustion-

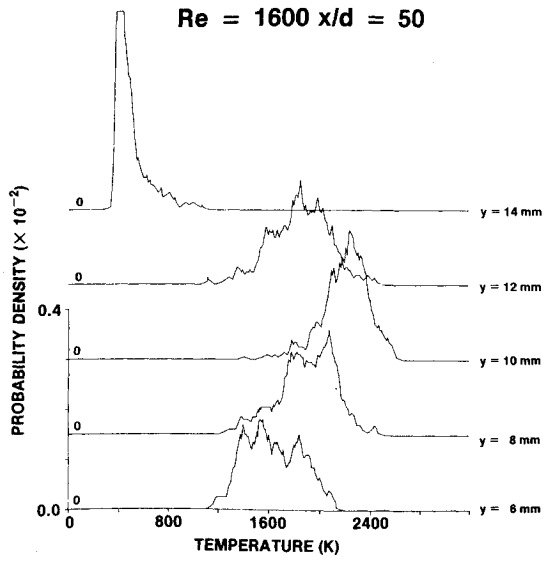

Fig. 12 Probability density functions of temperature measured in the transitional $Re=1600$ flame at various radial positions at $x/d=50$.

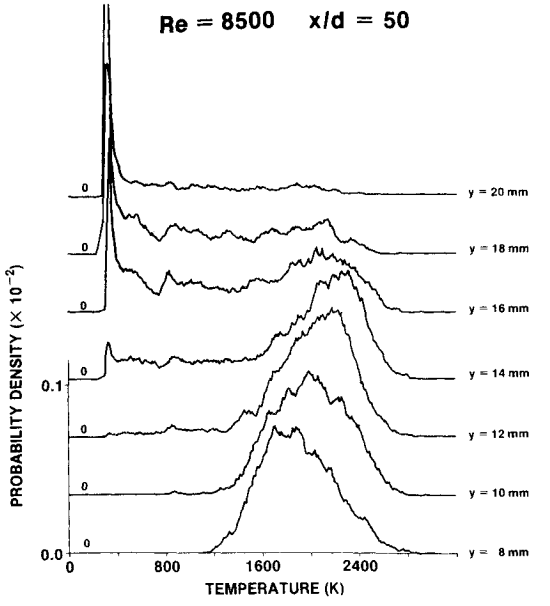

Fig. 13 Probability density functions of temperature measured in the turbulent $Re=8500$ flame at various radial positions at $x/d=50$.

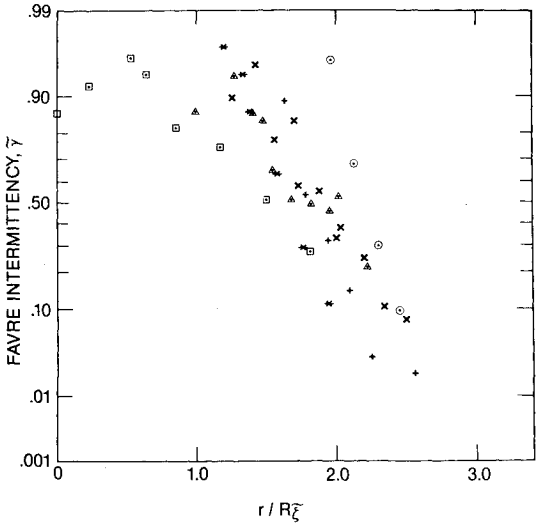

Fig. 14 Radial dependence of Favre intermittency from Raman data in the $Re=8500$ flame: ⊙ $x/d=10$, + $x/d=25$, * $x/d=50$, x $x/d=100$, △ $x/d=150$, ⊡ $x/d=200$.

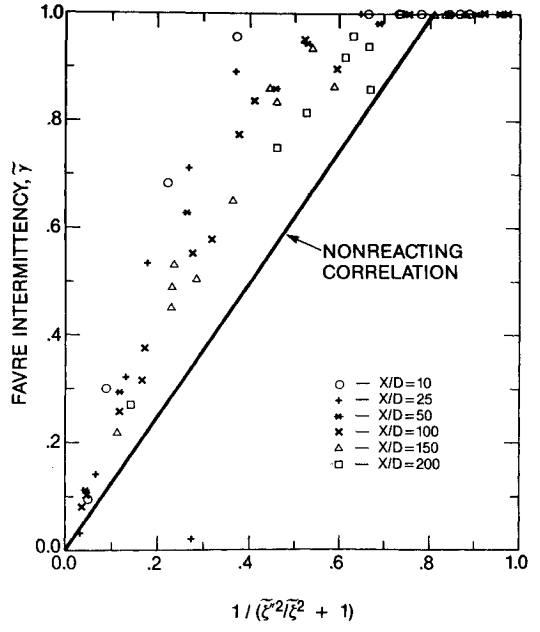

Fig. 15 Correlation of Favre intermittency with Favre mixture fraction fluctuation intensity from Raman measurements in the $Re=8500$ flame. Solid line is correlation by Kent and Bilger[49] from nonreacting flow data.

induced density changes. This is in contrast to the results of Schefer and Dibble[37] who found similarity in intermittency and density profiles in an H_2/argon flame, but their results may be a consequence of the much higher jet momentum in the H_2/argon flame.

It has been assumed in some conserved scalar modeling approaches[4,5,49] that the Favre intermittency can be related to $\tilde{\xi}''^2/\tilde{\xi}^2$ using an empirical correlation derived by Kent and Bilger[49] from measurements in near isothermal flows. This correlation is shown as a solid line in Fig. 15 with a slope of 1.25. The present experimental results in the $Re=8500$ H_2 diffusion flame show a slope greater than 1.25 with a systematic decrease in slope with increasing axial location (i.e., slope of 2.9 at $x/d=10$ and of 1.8 at $x/d=200$ using measurements from $\tilde{\gamma}=0$-0.8 and requiring that the curves go through the origin). The present data show marked nonlinearity for $\tilde{\gamma}>0.8$. The measured slopes are much higher than that found by Antonia and Bilger[28] in a nonreacting coflowing jet (slope of ~1.1), but are in reasonable agreement with the cold-flow jet into still air data of Becker et al.[57] and with the H_2/argon flame results of Schefer and Dibble[37] (slope of ~2.2).

Once the pdf from a point in the flow has been separated into individual pdf's for the turbulent and nonturbulent parts of the flow, each part can be separately analyzed to produce the conditional averages and higher-order moments.[58] The present $Re=8500$ data have been analyzed using conditional averaging; more detailed results are discussed elsewhere.[54,62] Such measurements of intermittency and conditional moments[54] are needed to compare with models[59,60] that separately describe turbulent and nonturbulent fluids. The major conclusion from such an analysis is that all of the pdf's of conserved and reactive scalars (for example, see Fig. 13) show a continuous distribution between turbulent and nonturbulent fluids and the turbulent pdf is distinctly non-Gaussian. This is also seen in pdf's from

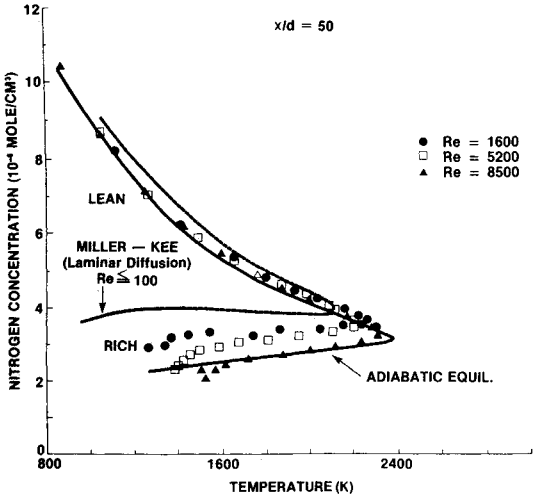

Fig. 16 Correlation of average values of N_2 concentration and temperature conditioned on measured mixture fraction from Raman data in the $Re = 1600$, 5200, and 8500 flames at $x/d = 50$. Compared to correlation calculated from an adiabatic equilibrium thermodynamic calculation[8] (solid line) and from a laminar H_2/air flame method[64] (dashed line).

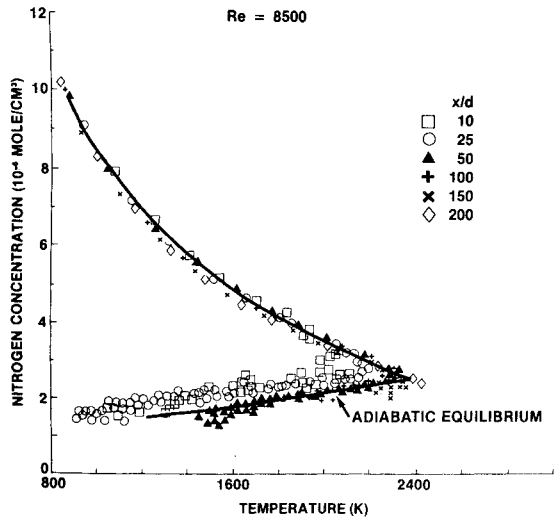

Fig. 17 Correlation of average values of N_2 concentration and temperature conditioned on measured mixture fraction from Raman data at various axial positions in the $Re = 8500$ flame.

nonreacting flows[58] and in reacting flows using other techniques.[50,53] Effelsburg and Peters[61] suggest that the measured pdf shapes indicate the importance of a third component (called the viscous superlayer) lying between the turbulent and nonturbulent zones. They have proposed a three-zone model, mathematically dividing the turbulent part of the pdf into a superlayer and a fully turbulent part. Based upon data from nonreacting wakes, they calculate that the superlayer can contribute up to 60% of the total flow. Similar analysis of the present H_2 diffusion flame data[62] show even larger apparent superlayer contributions.

VI. Identification of Important Processes (Differential Diffusion and Finite Rate Chemisty)

A major objective of these experiments has been to identify and quantify important processes in nonpremixed flames. Previously, the Raman measurements at $Re = 1600$ and 5200 were presented[7,8] in terms of correlation plots between the nitrogen concentration and temperature and compared with the adiabatic equilibrium correlation curve calculated assuming no heat loss from the flame, equal diffusion of species within the flame, and infinitely fast chemical reaction rates. A plot, similar to that published earlier,[8] is shown in Fig. 16. Here, however, the Raman data have been averaged in small mixture fraction intervals (rather than in temperature intervals) and data for the $Re = 8500$ flame have been added. The substantial deviations between the data and the adiabatic equilibrium calculation, particularly in the rich zones, were caused by differential molecular diffusion effects,[8] which had not been observed previously in turbulent flame experiments. This was confirmed by both comparison to conserved scalar modeling by Bilger,[63] which included molecular diffusion effects using perturbation analysis, and by detailed model/experiment comparisons.[4] Also shown in Fig. 16 is the correlation calculated for laminar H_2/air diffusion flames by Miller and Kee[64] corresponding to a Reynolds number of less than 100. The data in Fig. 16 (and the conserved scalar modeling[4,63]) demonstrate that differential diffusion effects are largest in laminar flames and become relatively unimportant in H_2 turbulent jet diffusion flames (at least at this x/d location) at Reynolds numbers greater than 8500.

Departures from the classical "fast chemistry" assumption are expected to be small in typical laboratory H_2/air turbulent diffusion flames and have been predicted using a perturbation analysis[65] or a two-scalar pdf approach.[66,67] Specific predictions of the effect of finite-rate chemistry in the $Re = 1600$ and 8500 flames indicate effects on the unconditioned mean temperature of -5 and -40 K, respectively, at $x/d = 50$.[4] Further analysis of the Raman data for the $Re = 8500$ flame is shown in Fig. 17, where data at $x/d = 10$-200 are plotted. The $x/d = 50$ data in Fig. 17 are the same as shown in Fig. 16, except that averages were obtained in narrower mixture fraction intervals. Clearly, no deviations from the adiabatic equilibrium theory are evident in the lean-flame zones or in the rich-flame zones at $x/d \geq 50$. However, small deviations are evident in rich zones at $x/d = 10$ and 25 and largest deviations occur for near stoichiometric mixture fractions at the nose of the curve in Fig. 17. Table 2 lists the *maximum* mean temperature conditioned on mixture fraction measured in the turbulent $Re = 8500$ flame as a function of x/d. The maximum adiabatic H_2/air flame temperature determined from an equilibrium flame calculation is 2380 K. Based upon extensive calibrations in laminar premixed H_2/air flames, temperature measurements made with the present pulsed Raman apparatus have a 4% relative standard deviation and an average temperature accuracy of ± 50 K. Thus, the Raman measurements agree within experimental error with the adiabatic equilibrium value at $x/d \geq 100$. However, the deviations closer to the nozzle are over 200 K, much larger than expected from experimental error. Although they could be due to inadequate spatial resolution of the Raman measurements close to the nozzle, these deviations are more likely due to the formation of superequilibrium concentrations of free radical (a finite-rate chemistry effect which lowers the flame temperature).

The values in Table 2 are *qualitatively* consistent with turbulent combustion model predictions,[65-67] which suggests that the amount of superequilibrium should be largest close to the nozzle and decrease farther downstream. Using a partial equilibrium thermodynamic calculation,[68] a temperature decrement ($T_{AE} - \tilde{T}$) of 270 K corresponds to an average OH concentration for a stoichiometric H_2/air mixture that is ~ 2.5 times its equilibrium value. Such large superequilibrium OH concentrations have been measured directly in the same H_2 flames using single-pulse OH laser saturated fluorescence and are reported in detail elsewhere.[68] Because of inaccuracies in the Raman temperature measurements and the relative insensitivity of temperature to superequilibrium effects, *quantitative* evaluations of finite-rate chemistry effects in turbulent combustion models are best made by comparisons with the OH concentration measurements.

Table 2 Comparison of maximum measured temperatures conditioned on mixture fraction measured in the $Re=8500$ H_2/air flame[a]

x/d	Maximum temp, K	T_{AE}-maximum temp, K
10	2110	−270
25	2185	−195
50	2300	−80
100	2320	−40
150	2350	−30
200	2425	+45

[a]The maximum H_2/air flame temperature from adiabatic equilibrium theory is 2380 K.

However, the present Raman results suggest that finite-rate chemical kinetic effects occur in H_2/air turbulent jet diffusion flames even at relatively modest Reynolds numbers ($Re=8500$) and are qualitatively consistent with direct measurements of OH radical concentrations.

VII. Summary

Four H_2/air jet diffusion flames, including laminar ($Re=660$), transitional ($Re=1600$), and turbulent ($Re=5200$ and 8500) types, were studied using the laser diagnostic techniques of planar OH fluorescence imaging, laser velocimetry, and pulsed Raman scattering. The planar OH fluorescence technique selectively images reaction zones and, although large and varied reaction zone shapes were observed in the turbulent flames, "coherent" structures were not evident. Laser velocimetry and pulsed Raman scattering provides probability density functions of axial velocity, temperature, density, major species concentrations, and a conserved scalar (hydrogen element mixture fraction). Averages, rms fluctuations, and half-radii are calculated from the measured pdf's and compared with previous measurements in reacting and nonreacting jets. Centerline decays of excess axial velocity measured in the $Re=1600$ and 8500 flames paralleled those of the Favre mixture fraction. The fluctuation intensities of excess axial velocity and of Favre mixture fraction are the same in the $Re=8500$ flame with values of 0.18-0.20 at $x/d\leq 100$, in agreement with nonreacting jet data. Far downstream ($x/d>100$) in the turbulent flames, the fluctuation intensities increase to values found in nonreacting wakes (>0.3). Fluctuation intensities of excess axial velocity in the transitional $Re=1600$ flame are very low in the laminar zone ($x/d<25$), very large (~ 0.35) in the transition region ($25<x/d<50$), and intermediate (0.08-0.15) in the turbulent zone ($x/d\geq 100$). In the turbulent flames, the half-radii (based upon excess velocity) has been compared to that predicted by correlations for nonreacting coflowing jets at different values of $\bar{U}_j/\bar{U}_a$. The reacting coflowing jets are found to grow more slowly with distance and have a half-radius about 20% less than their nonreacting counterparts in the far field.

The estimates of turbulent Schmidt number (based upon ratios of half-radii of excess velocity and Favre mixture fraction) in the $Re=1600$ flame are in reasonable agreement with the value of 0.7 found in nonreacting turbulent jets, but in the turbulent $Re=8500$ flame the measured turbulent Schmidt number is approximately equal to or somewhat greater than one.

Average values of temperature are in good agreement with previous thermocouple measurements and the rms fluctuations agree with model predictions in similar turbulent H_2 flames. The rms fluctuation values of 500 K on the centerline and 750 K off axis measured in the $Re=8500$ flame are somewhat larger than those measured by the thermocouples in CH_4 turbulent jet flames or by Raman scattering in H_2/argon turbulent jet flames.

Probability density functions of axial velocity were not bimodal in any of the flames studied, nor were the pdf's of the other variables in the transitional $Re=1600$ flame. However, in the mixing layer regions of the turbulent ($Re=5200$ and 8500) flames, the pdf's were bimodal—consisting of a sharp spike due to the freestream air and a broad peak due to the turbulent fluid. A continuous distribution between the nonturbulent and turbulent peaks was observed, similar to that found in nonreacting flows, which may indicate the importance of a broad superlayer region. The Favre intermittency profiles are Gaussian with the standard deviation of the interface becoming larger as x/d increases—perhaps indicating a trend from jet-like to wake-like behavior. The correlation of Favre intermittency with $(\tilde{\xi}''^2)^{1/2}/\tilde{\xi}^2$ is in agreement with that found in nonreacting jet flows in still air and in turbulent H_2/argon jet flames, indicating that $\tilde{\gamma}=2.2$ $(\tilde{\xi}''^2/\tilde{\xi}^2+1)^{-1}$, but differs somewhat from that found in nonreacting coflowing jets.

Correlations of nitrogen concentrations and temperature conditioned on mixture fraction suggest that preferential diffusion of H_2 is important in the transitional flames, but of little importance at $Re\geq 8500$. However, the formation of superequilibrium amounts of free radicals (a finite-rate chemistry effect) is found to be significant close to the nozzle in the turbulent $Re=8500$ flame, but of decreasing significance farther downstream.

Acknowledgments

The authors acknowledge the partial support of this research by the U.S. Department of Energy and the Office of Naval Research and helpful discussions with S. Correa (General Electric), R. W. Dibble (Sandia National Laboratories), and R. W. Bilger (University of Sydney). The technical expertise of F. Haller contributed greatly to this work.

We are grateful for the collaboration of R. Hanson, G. Kychakoff, and R. Howe (Stanford University) for the planar OH fluorescence experiments and to C. M. Penney for work on the development of the pulsed Raman apparatus.

References

[1]Libby, P. A. and Williams, F. A., (eds.), *Turbulent Reacting Flows*, Springer-Verlag, New York, 1980.

[2]Kollmann, W. (ed.), *Prediction Methods for Turbulent Flows*, Hemisphere Publishing Co., New York, 1980.

[3]Jones, W. P. and Whitelaw, J. H., "Calculation Methods for Turbulent Reacting Flows: A Review," *Combustion and Flame*, Vol. 48, 1982, p. 1.

[4]Drake, M. C., Bilger, R. W., and Starner, S. H., "Raman Measurements and Conserved Scalar Modeling in Turbulent Diffusion Flames," *Nineteenth Symposium (International) on Combustion*, The Combustion Institute, Pittsburgh, PA, 1982, p. 459.

[5]Bilger, R. W., "Turbulent Flows with Nonpremixed Reactants," *Turbulent Reacting Flows*, edited by P. A. Libby and F. A. Williams, Springer-Verlag, New York, 1980, p. 65.

[6]Eckbreth, A.E., "Recent Advances in Laser Diagnostics for Temperature and Species Concentrations in Combustion," *Eighteenth Symposium (International) on Combustion* The Combustion Institute, Pittsburgh, PA, 1981, p. 1471.

[7]Drake, M. C., Lapp, M., Penney, C. M., Warshaw, S., and Gerhold, B. W., "Measurements of Temperature and Concentration Fluctuations in Turbulent Diffusion Flames Using Pulsed Raman Spectroscopy," *Eighteenth Symposium (International) on Combustion*, The Combustion Institute, Pittsburgh, PA, 1981, p. 1521.

[8]Drake, M. C., Lapp, M., Penney, C. M., Warshaw, S., and Gerhold, B.W., "Probability Density Functions and Correlations of Temperature and Molecular Concentrations in Turbulent Diffusion Flames," AIAA Paper 81-0103, 1981.

[9]Kychakoff, G., et al., "Visualization of Turbulent Flame Fronts Using Planar Laser-Induced Fluorescence," *Science*, Vol. 224, 1984, p. 382.

[10]Drake, M. C., Lapp, M., and Penney, C. M., "Use of the Raman Effect for Gas Temperature Measurements," *Temperature, Its Measurement and Control in Science and Industry*, Vol. 5, edited by J. F. Schooley, American Insitute of Physics, New York, 1982, p. 631.

[11]Drake, M. C., Lapp, M., Pitz, R. W., and Penney, C. M., "Dynamic Measurements of Gas Properties by Vibrational Raman

Scattering: Application to Flames," *Time Resolved Vibrational Spectroscopy*, edited by G. H. Atkinson, Academic Press, New York, 1983, p. 83.

[12]Lapp, M., Drake, M. C., Penney, C. M., Pitz, R. W., and Correa, S., "Turbulent Combustion Experiments and Modeling," General Electric Co., Schenectady, NY, Rept. 83CRD049, 1983; (also final Rept. DoE/ET/13146-T14, Sept. 1983, available from NTIS, Order No. DE84-002806).

[13]Kent, J. H. and Bilger, R. W., "Turbulent Diffusion Flames," *Fourteenth Symposium (International) on Combustion*, The Combustion Institute, Pittsburgh, PA, 1973, p. 615.

[14]Kent, J. H. and Bilger, R. W., "Measurements in Turbulent Jet Diffusion Flames," Mechanical Engineering Dept., University of Sydney, Sydney, Australia, Rept. TN-F-41, Oct. 1972.

[15]Rohsenow, W. N. and Choi, H. Y., *Heat, Mass and Momentum Transfer*, Prentice Hall, Englewood Cliffs, NJ, 1961, p. 74.

[16]Takeno, T. and Kotani, Y., "An Experimental Study on the Stability of Jet Diffusion Flame," *Acta Astronautica*, Vol. 2, 1975, p. 999.

[17]Takeno, T. and Kotani, Y., "Transition and Structure of Turbulent Jet Diffusion Flames," *Turbulent Combustion, Progress in Astronautics and Aeronautics*, Vol. 58, edited by L. A. Kennedy, AIAA, New York, 1978, p. 19.

[18]Hottel, H. C. and Hawthorne, W. R., "Diffusion in Laminar Flame Jets," *Third Symposium (International) on Combustion*, Williams and Wilkins, Baltimore, MD, 1953, p. 254.

[19]Takagi, T., Shin, H., and Ishio, A., "Local Laminarization in Turbulent Diffusion Flames," *Combustion and Flame*, Vol. 37, 1980, p. 163.

[20]Williams, F. A., "Recent Advances in Theoretical Descriptions of Turbulent Diffusion Flames," *Turbulent Mixing in Nonreactive and Reactive Flows*, edited by S.N.B. Murthy, Plenum Press, New York, 1974, p. 189.

[21]Peters, N., "Laminar Diffusion Flamelet Models in Nonpremixed Turbulent Combustion," *Progress in Energy in Combustion Science*, Vol. 10, 1984, p. 319.

[22]Roshko, A., "Structure of Turbulent Shear Flows: A New Look," *AIAA Journal*, Vol. 14, 1976, p. 1349.

[23]Peters, N. and Williams, F. A., "Coherent Structures in Turbulence Combustion," *Modeling Turbulence and Mixing, Lecture Notes in Physics*, Vol. 136, edited by J. Jimenez, Springer-Verlag, Berlin, FRG, 1981, p. 364.

[24]Yule, A. J., "Large-Scale Structure in the Mixing Layer of a Round Jet," *Journal of Fluid Mechanics*, Vol. 89, 1978, p. 413.

[25]Townsend, A. A., *The Structure of Turbulent Shear Flow*, Cambridge Press, Cambridge, England, 1956.

[26]Glass, M. G. and Bilger, R. W., "The Turbulent Jet Diffusion Flame in a Co-Flowing Stream—Some Velocity Measurements," *Combustion Science and Technology*, Vol. 18, 1978, p. 165.

[27]Rodi, W. (ed.), *Turbulent Bouyant Jets and Plumes*, Pergamon Press, New York, 1982.

[28]Antonia, R. A. and Bilger, R. W., "The Heated Round Jet in a Co-Flowing Stream," *AIAA Journal*, Vol. 14, 1976, p. 1541.

[29]Uberoi, M. and Freymuth, P., "Turbulent Energy Balance and Spectra of the Axisymmetric Wake," *The Physics of Fluids*, Vol. 13, 1970, p. 2205.

[30]Gibson, C. H., Chen, C. C., and Lin, S. C., "Measurements of Turbulent Velocity and Temperature Fluctuations in the Wake of a Sphere." *AIAA Journal*, Vol. 6, 1968, p. 642.

[31]Freymuth, P. and Uberoi, M. S., "Temperature Fluctuations in the Turbulent Wake Behind an Optically Heated Sphere," *The Physics of Fluids*, Vol. 16, 1973, p. 161.

[32]Starner, S. H. and Bilger, R. W., "LDA-Measurements in a Turbulent Diffusion Flame with Axial Pressure Gradients," *Combustion Science and Technology*, Vol. 21, 1980, p. 259.

[33]Starner, S. H., "Joint Measurements of Radial Velocity and Scalars in a Turbulent Diffusion Flame," *Combustion Science and Technology*, Vol. 30, 1983, p. 145.

[34]Starner, S. H., "Investigation of Turbulent Diffusion Flames," Ph.D. Thesis, University of Sydney, Sydney, Australia, 1980.

[35]Starner, S. H. and Bilger, R.W., "Measurement of Scalar-Velocity Correlations in a Turbulent Diffusion Flame," *Eighteenth Symposium (International) on Combustion*, The Combustion Institute, Pittsburgh, PA, 1981, p. 921.

[36]Driscoll, J. F., Schefer, R. W., and Dibble, R. W., "Mass Fluxes $\rho'u'$ and $\rho'v'$ Measured in a Turbulent Nonpremixed Flame," *Nineteenth Symposium (International) on Combustion*, The Combustion Institute, Pittsburgh, PA, 1982, p. 477.

[37]Schefer, R. W. and Dibble, R. W., "Simultaneous Measurements of Velocity and Density in a Turbulent Nonpremixed Flame," Sandia National Laboratories Rept. SAND 82-8810, July 1983 (also AIAA Paper 83-0401, Jan. 1983).

[38]Dibble, R. W., Kollmann, W., and Schefer, R. W., "Conserved Scalar Fluxes Measured in a Turbulent Nonpremixed Flame by Combined Laser Doppler Velocimetry and Laser Raman Scattering," *Combustion and Flame*, Vol. 55, 1984, p. 307.

[39]Dibble, R. W. and Schefer, R. W., "Simultaneous Measurement of Velocity and Scalars in Turbulent Nonpremixed Flames by Combined Laser Doppler Velocimetry and Laser Raman Scattering," *Fourth Symposium on Turbulent Shear Flows*, Karlsruhe, FRG, Sept. 1983, (also Sandia National Laboratories, Rept. SAND83-8772).

[40]Kent, J. H., "Turbulent Jet Diffusion Flames," Ph.D. Thesis, University of Sydney, Sydney, Australia, 1972.

[41]Kennedy, I. M. and Kent, J. H., "Scalar Measurements in a Co-Flowing Turbulent Diffusion Flame," *Combustion Science and Technology*, Vol. 25, 1981, p. 109.

[42]Wygnanski, I. and Fiedler, H., "Some Measurements in the Self-Preserving Jet," *Journal of Fluid Mechanics*, Vol. 38, 1969, p. 577.

[43]Birch, A. D., Brown, D. K., Dodson, M. G., and Thomas, J. R., "The Turbulent Concentration Field of a Methane Jet," *Journal of Fluid Mechanics*, Vol. 88, 1978, p. 431.

[44]Abramovich, G. N., *Theory of Turbulent Jets*, MIT Press, Cambridge, MA, 1963.

[45]Antonia, R. A. and Bilger, R. W., "An Experimental Investigation of an Axisymmetric Jet in a Co-Flowing Air Stream," *Journal of Fluid Mechanics*, Vol. 61, 1973, p. 805.

[46]Pitz, R. W. and Daily, J. W., "Combustion in a Turbulent Mixing Layer Formed at a Rearward Facing Step," *AIAA Journal*, Vol. 21, 1983, p. 1565.

[47]Steward, F. R. and Guruz, A. G., "Aerodynamics of a Confined Jet with Variable Density," *Combustion Science and Technology*, Vol. 16, 1977, p. 29.

[48]Batt, R. G., "Turbulent Mixing of Passive and Chemically Reacting Species in a Low-Speed Shear Layer," *Journal of Fluid Mechanics*, Vol. 82, 1977, p. 53.

[49]Kent, J. H. and Bilger, R. W., "The Prediction of Turbulent Diffusion Flame Fields and Nitric Oxide Formation," *Sixteenth Symposium (International) on Combustion*, The Combustion Institute, Pittsburgh, PA, 1977, p. 1643.

[50]Roberts, P. T. and Moss, J. B., "A Wrinkled Flame Interpretation of the Open Turbulent Diffusion Flame," *Eighteenth Symposium (International) on Combustion*, The Combustion Institute, Pittsburgh, PA, 1981, p. 941.

[51]Lockwood, F. C. and Moneib, H. A., "Fluctuating Temperature Measurements in Turbulent Jet Diffusion Flame," *Combustion and Flame*, Vol. 47, 1982, p. 291.

[52]Lockwood, F. C. and Odidi, A. O., "Measurement of Mean and Fluctuating Temperature and of Ion Concentration in Round Free-Jet Turbulent Diffusion and Premixed Flames," *Fifteenth Symposium (International) on Combustion*, The Combustion Institute, Pittsburgh, PA, 1975, p. 561.

[53]Dibble, R. W. and Hollenbach, R. E., "Laser Rayleigh Thermometry in Turbulent Flames," *Eighteenth Symposium (International) on Combustion*, The Combustion Institute, Pittsburgh, 1981, p. 1489.

[54]Pitz, R. W. and Drake, M. C., "Intermittency and Conditional Averaging in a Turbulent Nonpremixed Flame by Raman Scattering," AIAA Paper 84-0197, 1984, *AIAA Journal*, to be published.

[55]Antonia, R. A., Prabhu, A., and Stephenson, S. E., "Conditionally Sampled Measurements in a Heated Turbulent Jet," *Journal of Fluid Mechanics*, Vol. 72, 1975, p. 455.

[56]Demetriades, A., "Turbulent Front Structure of an Axisymmetric Compressible Wake," *Journal of Fluid Mechanics*, Vol. 34, 1968, p. 465.

[57]Becker, H. A., Hottel, H. C., and Williams, G. C., "The Nozzle-Fluid Concentration Field of the Round Turbulent, Free Jet," *Journal of Fluid Mechanics*, Vol. 30, 1967, p. 285.

[58]Libby, P. A., Chigier, N., and LaRue, J. C., "Conditional Sampling in Turbulent Combustion," *Progress in Energy and Combustion Science*, Vol. 8, 1982, p. 203.

[59]Pope, S. B., "Calculations of a Plane Turbulent Jet," AIAA Paper 83-0286, 1983.

[60]Kollmann, W., "The Prediction of the Intermittency Factor for Turbulent Shear Flows," AIAA Paper 83-0382, 1983.

[61]Effelsburg, E. and Peters, N., "A Composite Model for the Conserved Scalar Pdf," *Combustion and Flame*, Vol. 50, 1983, p. 351.

[62]Drake, M. C., Shyy, W., and Pitz, R. W., "Superlayer Contributions to Conserved Scalar Pdfs in an H_2 Turbulent Jet Diffusion Flame," *Journal of Fluid Mechanics*, to be published.

[63]Bilger, R. W., "Molecular Transport Effects in Turbulent Diffusion Flames at Moderate Reynolds Numbers," *AIAA Journal*, Vol. 20, 1982, p. 962.

[64]Miller, J. A. and Kee, R. J., "Chemical Nonequilibrium Effects in Hydrogen-Air Laminar Jet Diffusion Flames," *Journal of Physical Chemistry*, Vol. 61, 1977, p. 2534.

[65]Bilger, R. W., "Perturbation Analysis of Turbulent Nonpremixed Combustion," *Combustion Science and Technology*, Vol. 22, 1980, p. 251.

[66]Janicka, J. and Kollmann, W., "A Two-Variable Formalism for the Treatment of Chemical Reactions in Turbulent H_2-Air Diffusion Flames," *Seventh Symposium (International) on Combustion*, The Combustion Institute, Pittsburgh, PA, 1979, p. 421.

[67]Janicka, J. and Kollmann, W., "The Calculation of Mean Radical Concentrations in Turbulent Diffusion Flames," *Combustion and Flame*, Vol. 44, 1982, p. 319.

[68]Drake, M. C. et al., "Measurements of Superequilibrium Hydroxyl Concentrations in Turbulent Nonpremixed Flames Using Saturated Fluorescence," *Twentieth Symposium (International) on Combustion*, 1985, p. 327.